RMetS
Royal Meteorological Society

# On the severe convective storm of 29 October 2013 in the Balearic Islands: observational and numerical study

R. Romero,* C. Ramis and V. Homar

*Meteorology Group, Departament de Física, Universitat de les Illes Balears, Palma de Mallorca, Spain*

*Correspondence to: R. Romero, University of the Balearic Islands, Physics, Ctra Valldemossa, km 7.5, Palma de Mallorca, Illes Balears 07122, Spain. E-mail: romu.romero@uib.es

**On 29 October 2013, a severe squall line developed to the west of the Balearic Islands (Spain) ahead of an advancing cold front and then crossed the archipelago. We first provide an observational characterization of the event based on surface reports, remote sensing products, radiosoundings and synoptic information. We also achieve, by means of numerical experiments, new insights into the kinematic and thermodynamic factors that governed the genesis and evolution of the linear convective system. Radar and satellite images confirm the fast movement and linear shape of the system, with an indication of a possible transition into a bow-echo structure during its later stages. The synoptic setting at mid-upper tropospheric levels was dominated by a cold trough extended over western Europe, associated with a jet stream located downstream. Convection evolved under the right entrance region of the jet and initiated under the crucial influence of a surface low that developed over the Mediterranean Sea ahead of the cold front. The low not only cooperated with the upper-level dynamical forcing to erode a capping inversion initially present over the Balearics and moisten the atmospheric column above, but also shaped and enhanced a convergence line along which the first convective cells grew and self-aggregated. This scenario is confirmed by numerical simulations of the case, which also emphasize the important role of regional topography in the production of the aforementioned maritime convergence through the mesoscale modulation of the low-level flow. Additional simulations show that (i) the destabilization of the low-level air mass necessary for triggering and feeding an organized convective system on 29 October 2013 was attributable to prior evaporation from the Mediterranean and (ii) sea-surface temperatures appear to be critical for a successful fine-grid numerical forecast of the mode, degree of severity, timing and track of the convective precipitation system.**

*Key Words:* western Mediterranean; convective weather; squall line; bow echo; convergence line; topographic influence; SST influence; high-resolution simulation

*Received 11 April 2014; Revised 1 July 2014; Accepted 14 July 2014; Published online in Wiley Online Library*

## 1. Introduction

The development of high-impact weather events in the western Mediterranean region is not uncommon. Almost yearly, episodes of this type are recorded on the Mediterranean coasts and particularly in the Spanish sectors. Possibly the best known episodes in terms of their recurrence and negative consequences inflicted on material goods and human lives are heavy precipitation and subsequent flash floods, most frequent in the autumn (Tudurí and Ramis, 1997; Romero *et al.*, 1998a). Historical references to heavy precipitation events are numerous, some of these going back to the Middle Ages (e.g. Barceló, 1991). In this context, the province of Valencia (eastern Spain) possesses one of the highest daily accumulations ever recorded in Europe, 817 mm on 3 November 1987 (Ramis *et al.*, 2013). Two of the greatest flash-flood-producing storms in Valencia region during the last decades, associated with circular-shaped meso-$\beta$ convective systems, were thoroughly analyzed by Romero *et al.* (2000) and Fernández *et al.* (1995) using mesoscale numerical modelling. They found the primary role of shallow low-pressure systems on the localization and feeding of the precipitation systems. Other numerical studies of heavy precipitation cases have shown the importance of synergy between evaporation from the sea and local orography (Romero *et al.*, 1997, 1998b; Duffourg and Ducrocq, 2011; Malguzzi *et al.*, 2006, among others) or the essential role of the north African mountain chains in generating or enhancing low-level convergence over the Mediterranean Sea, which becomes instrumental in triggering the convection (e.g. Homar *et al.*, 1999). In addition to heavy rain, other convective severe phenomena like tornadoes (Homar *et al.*, 2001; Gayà, 2011), hail

(Sánchez *et al.*, 2003) and squall lines (Ramis *et al.*, 1997, 1999, 2009; Ducrocq and Bougeault, 1995) occasionally occur.

Squall lines that affected the Balearic Islands in recent years have entailed serious disruptions and even substantial damage locally. The storm of 4 October 2007 affected the capital of the islands, Palma de Mallorca, killing one person and causing material losses estimated at 10 M€ (Ramis *et al.*, 2009). The storm of 3 October 2008 also affected the city of Palma, in the form of large-size hail, although reports of damage were scarce in this case. On 1 July 2012 a characteristic burst of heavy rain and strong winds accompanied the passage of another squall line. A similar severe weather situation unfolded on 29 October 2013. The analysis of that storm is the object of the present study.

All aforementioned squall lines had in common their initial development over the sea. Ramis *et al.* (2009) show that the convective organization of the 4 October 2007 event was influenced by the thermal structure and three-dimensional wind distribution found in the warm sector ahead of a kata-type cold front that was located over the Iberian Peninsula. The lack of meteorological data over maritime areas, especially in the development zones, confers an essential role on numerical tools for the diagnostic evaluation of the genesis and evolution of mesoscale convective systems (MCSs). In this way, Cohuet *et al.* (2011) presented a fine-grid simulation of the 4 October 2007 situation using the Meso-NH numerical model. The simulation revealed the crucial action of a convergence zone found at the lowest tropospheric levels off the southeast coast of the Iberian Peninsula in the convective initiation. In addition, the high horizontal resolution used (600 m) allowed the model to resolve the organized linear structure of the storm realistically.

The aim of this work is the analysis of the 29 October 2013 convective storm and the encompassing meteorological setting from a dual point of view: (i) interpretation of the available observations and (ii) investigation of the physical processes involved in the initiation and evolution of the squall line by making use of numerical simulations with the MM5 mesoscale model. A novel feature of the present study compared with the vast majority of post-event analysis of high-impact Mediterranean storms is the use of convection-resolving resolutions in the model and the emphasis on the regional and local factors

**Figure 1.** Photograph of the thunderstorm taken from Porto Colom on 29 October 2013 at 1515 UTC. The greenish colour along the horizon is evident.

responsible, individually or synergistically, for the generation and sustainment of low-level convergence and thermodynamic ingredients capable of initiating and maintaining the storm. The article is structured as follows: section 2 presents the event and its meteorological characteristics; section 3 analyzes the remote sensing observations (radar and satellite); section 4 presents the synoptic and subsynoptic scenario; section 5 is devoted to the numerical diagnosis of the simulations; and, finally, section 6 provides the main conclusions obtained in the study.

## 2. The event

On 29 October 2013 at about 1300 UTC, a thunderstorm irrupted over the Balearic Islands and led to notable social disruptions, owing to the associated extreme precipitation intensity, high lightning activity and strong winds. This event was preceded by an unusually dry and warm period in Mediterranean Spain: no rain occurred on the previous days and the month as a whole was abnormally dry and warm, in spite of October being the wettest month in the Islands according to climatology

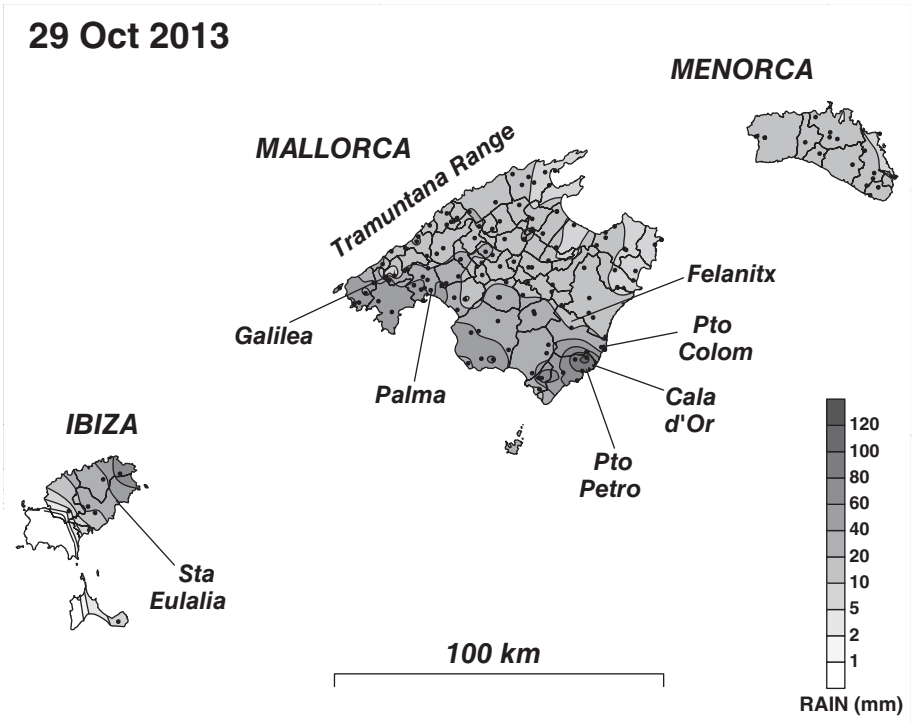


**Figure 2.** Spatial distribution of the rainfall recorded in the Balearic Islands on 29 October 2013 (dots indicate the position of the rain-gauge stations). Municipality divisions and locations mentioned in the text are indicated.

 

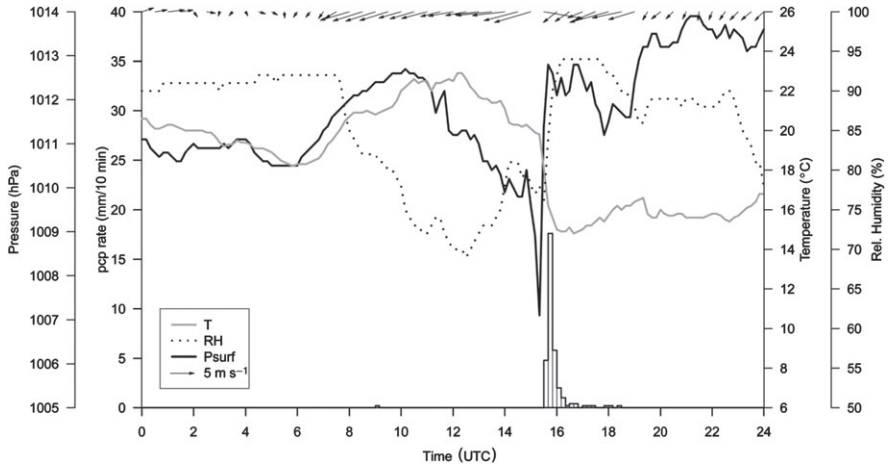


**Figure 3.** Meteogram at Porto Colom AEMET automatic weather station for 29 October 2013. Plotted vectors are 10 min average winds.

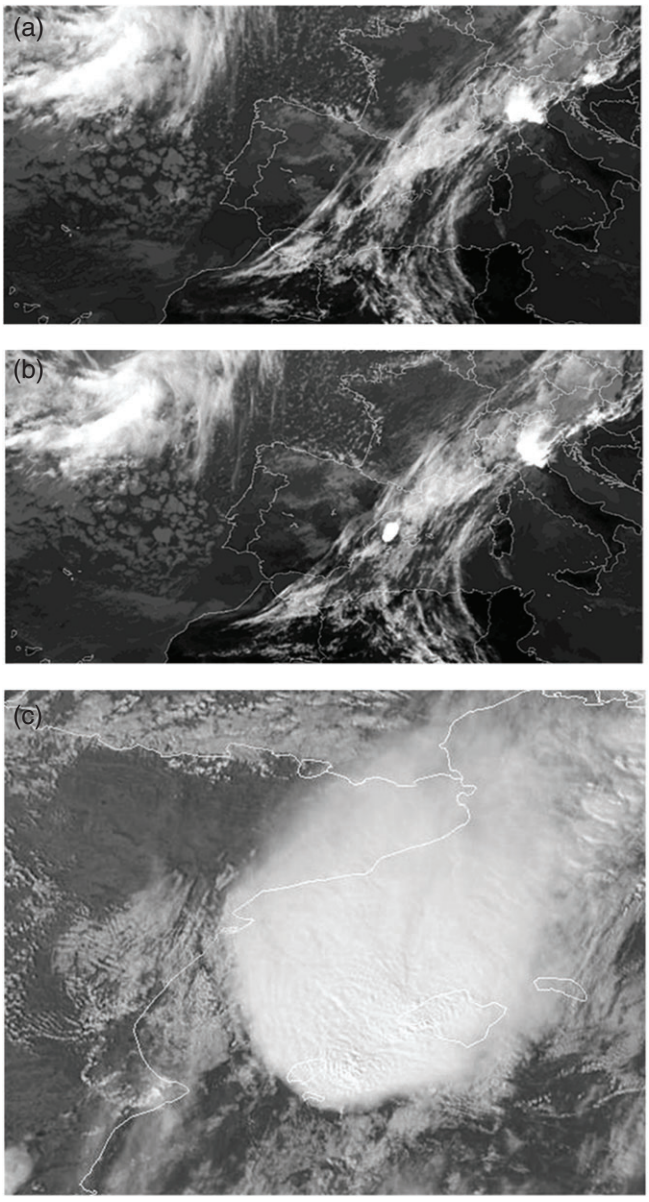


**Figure 4.** IR *Meteosat* images on 29 October 2013, at (a) 1000 UTC and (b) 1100 UTC. (c) Visible image at 1400 UTC.

(see http://www.aemet.es/documentos/es/serviciosclimaticos/vigilancia_clima/resumenes_climat/mensuales/2013/res_mens_clim_2013_10.pdf). As illustrative examples of the storm intensity, precipitation rates reached 25 mm in 20 min at Santa Eulalia (Ibiza), 20 mm in 10 min at Palma de Mallorca, 66 mm in 35 min at Galilea (Mallorca), 45 mm in 15 min at Felanitx (Mallorca) and as much as 260 mm $h^{-1}$ during some minutes at Porto Colom (Mallorca). Hailstones of about 2.5 cm in diameter were also observed at Porto Petro (Mallorca). The strong winds caused by the storm (gusts over 90 km $h^{-1}$) took many trees down and this affected contiguous residential homes and hotels, especially at tourist centres of southeast Mallorca such as Cala d'Or, Porto Colom and Porto Petro (see Figure 2 later for locations). In addition, beaches in these coastal localities were severely damaged by the sudden runoffs produced. No casualties occurred, although six persons had to be rescued when they were about to succumb to the floods. Total estimated insured losses produced by this thunderstorm were 15 M€.

Figure 1 shows the visual appearance of the convective cloud base as photographed from Porto Colom. The evident green tonality of a portion of the cloud is a feature occasionally observed in intense thunderstorms (Gallagher *et al.*, 1996; Wang, 2002) and was also seen in the 4 October 2007 case (Ramis *et al.*, 2009).

Total accumulated precipitation values over the Balearics are shown in Figure 2. These measurements correspond to 24 h accumulations collected at 0700 UTC on 30 October, but they were actually recorded during the short period of storm passage on the afternoon of 29 October. The greatest amounts were observed in north Ibiza and south Mallorca, especially in its southeast coastal lands, matching up with the areas affected by severe wind gusts.

The surface pressure time series from Porto Colom (Figure 3) shows the typical pattern of the passage of a squall line (Johnson and Hamilton, 1988). A pre-squall line meso-low, a meso-high associated with the thunderstorm downdraughts and a much shallower post-squall-line depression signal are all clearly identified. Temperature and humidity series indicate a decrease of 4.5 °C simultaneous to the arrival of the squall line and a short-lasting decrease in relative humidity, followed by an increase to almost saturation. The wind that was blowing from the northeast changed abruptly to the west-northwest and increased its magnitude during this time interval. The maximum recorded wind gust at this station was 61 km $h^{-1}$, but it exceeded 90 km $h^{-1}$ at the neighbouring Porto Petro site. Precipitation intensity peaked at 18 mm in 10 min as the meso-high passed over the Porto Colom station.

The above fluctuations of the surface variables, also observed at other stations in south Mallorca, and the kind of meteorological phenomena produced by the storm strongly suggest that a MCS with linear organization, namely a squall line, was the causative system of the severe weather episode in the Balearics on that day.

## 3. Remote sensing observations

*Meteosat* satellite images and especially the regional scans made by Valencia and Balearic Islands Agencia Estatal de Meteorología

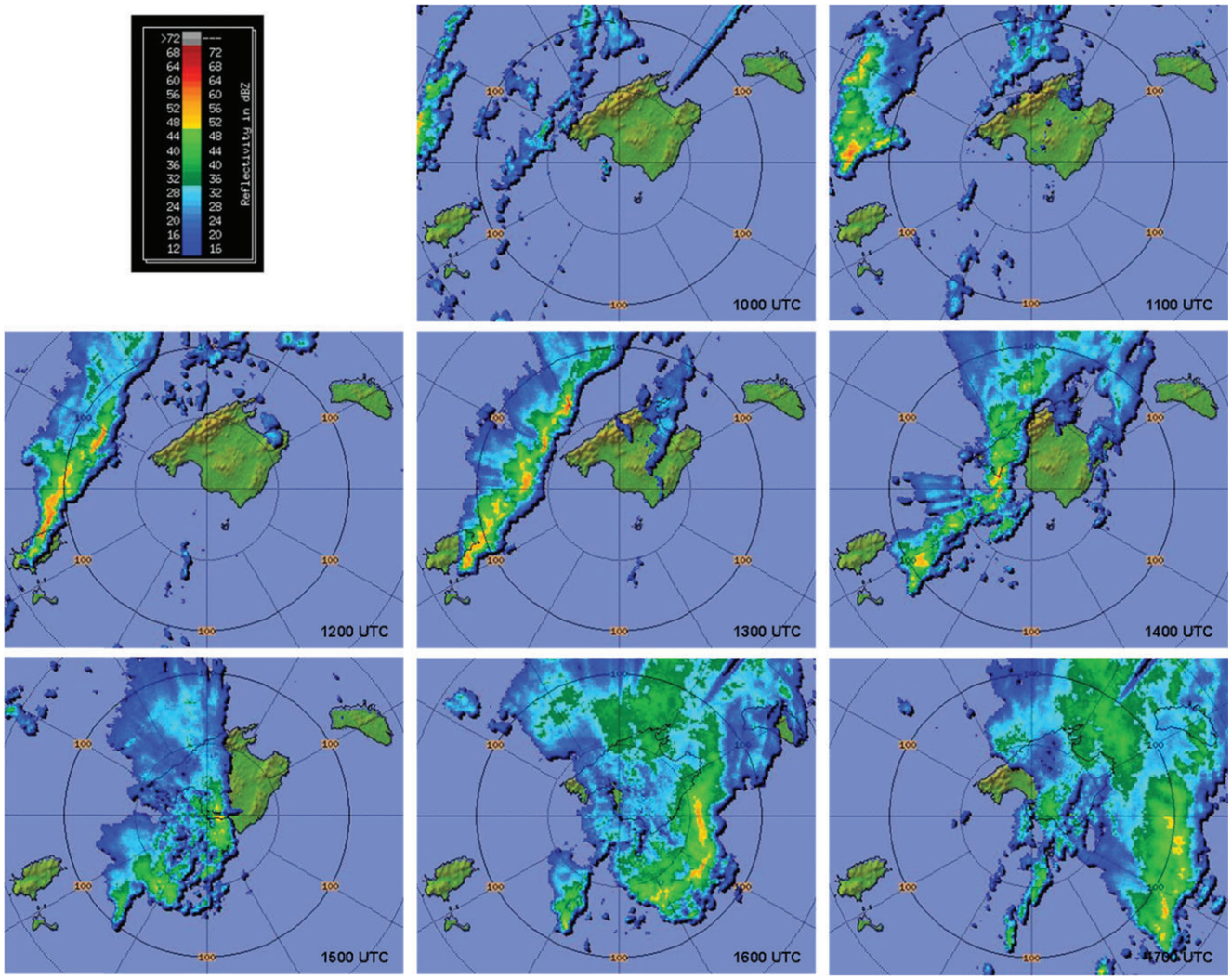


**Figure 5.** Hourly series for 29 October 2013 of reflectivity (dBZ) of CAPPI image (2.5 km height) from the Mallorca radar.

(AEMET) radars allowed the monitoring of the MCS from its genesis time until it left the Islands on its way to the east.

Satellite images show that at about 0930 UTC several convective nuclei formed between the Balearic Islands and the Iberian Peninsula. These initially separated convective elements grew very fast and finally joined together to form a coherent system extended in the vertical across the full troposphere. Figure 4 illustrates, over satellite images, the evolution of the system from the convection initiation phase until the complete development of the convective system. The system remained stationary during the entire development phase and then started to progress eastwards. The visible channel image reveals the power of the convection perfectly: overshooting tops on the deepest convective cells as well as the characteristic gravity waves radiating away from the thunderstorms in response to the updraughts punching on the tropopause.

Constant Altitude Plan Position Indicator (CAPPI) images at 2.5 km altitude from the radar at the Balearic Islands reveal a linear precipitation structure during the initiation phase, occurring about 120 km to the west of Mallorca (Figure 5) and about 100 km ahead of the cold front that was crossing the Iberian Peninsula (discussed in the next section). Radar images also show that this precipitation line remained almost stationary for about 1 h and then started to move eastwards at an estimated speed of about 40 km $h^{-1}$. As it progressed toward the Islands, new convective cells were built within the line. It acquired the most clear elongated shape around 1230 UTC, while crossing the northern part of Ibiza. Precipitation intensity within the line was very important, as revealed by reflectivity values as high as 60–70 dBZ. Later on, the convective line lost its morphological identity when interacting with the Mallorcan topography. At around 1530 UTC, the images do not show a well-defined linear structure, although the occurrence of convective cells that preserve the abovementioned extreme reflectivity values is still evident. Regarding the squall-line structure, bow echo signatures (Johns, 1993) can be identified at some times, but especially at 1600 UTC. Rear inflow notches (Przybylinski, 1995) are effectively detected on some images throughout the life of the storm. The maximum reflectivity product (Figure 6) reveals that five distinct cells formed during the initiation phase of the squall line. A multicellular convective structure – with no signatures of severity – is identified during the first hours. Only during the last stages is a weak echo region visible, on both zonal and meridional projections, in the convective cell located over the southeastern Mallorcan coast (Figure 6(b)). That cell produced the largest impacts registered for this episode. The signal from the Valencia radar confirms this description, especially with regard to the position of the initial convective clusters.

Unfortunately, no Doppler information is available to obtain a dynamical picture of the wind field associated with the squall line.

## 4. Meteorological setting

The large-scale meteorological state prior to the development of the squall line was characterized, at the surface, by the presence of a subtropical anticyclone to the west of the Iberian Peninsula, directly affecting its western half (Figure 7(a)). Low-pressure systems were positioned at relatively high latitudes, inducing a basic westerly flow over most of Europe. Such a dominant zonal circulation was, however, broken over the western Mediterranean, which lay under the influence of low

 

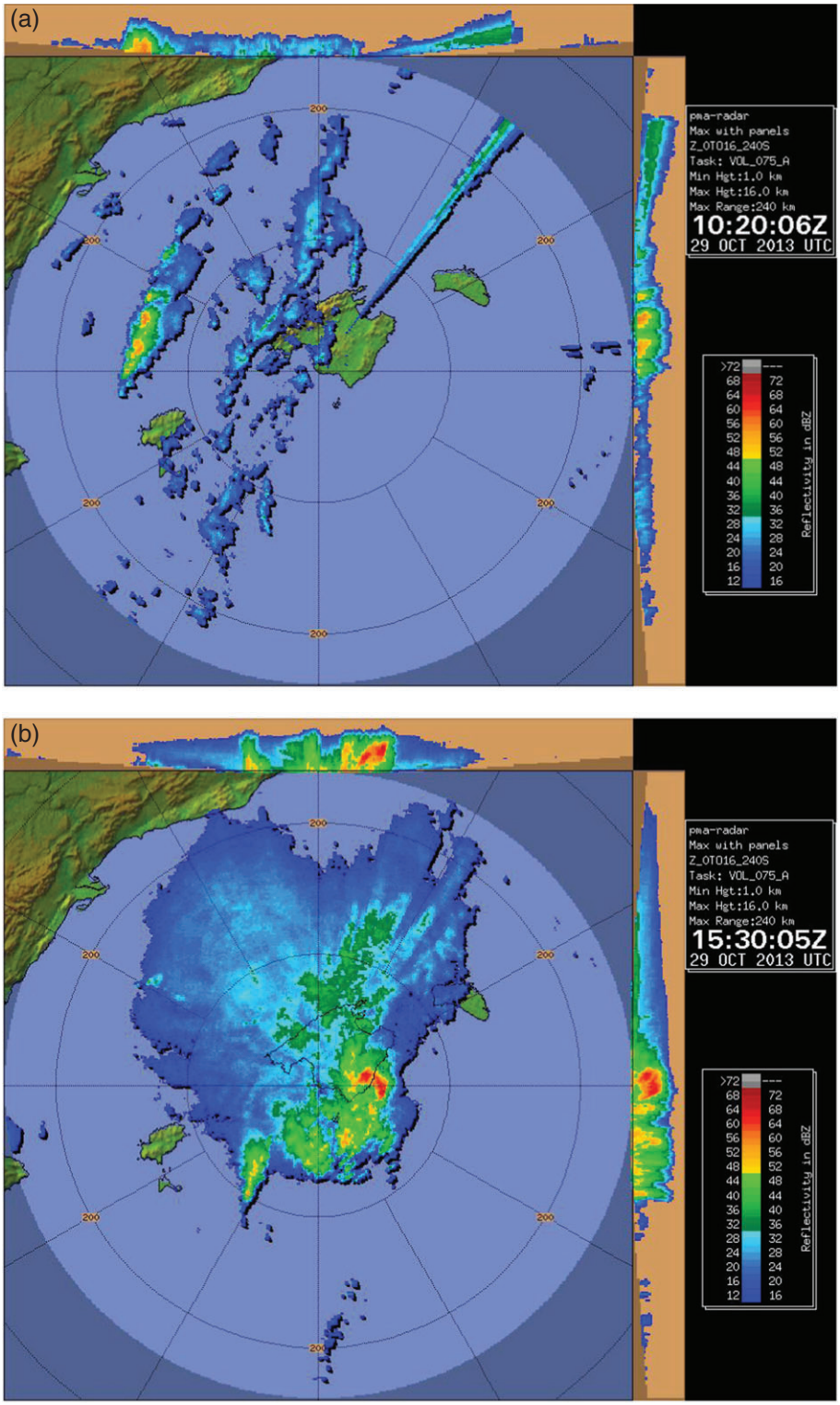


**Figure 6.** Map of maximum reflectivity and its zonal and meridional vertical projections (dBZ) for 29 October 2013 from the Mallorca radar, at (a) 1020 UTC and (b) 1530 UTC.

pressures. A cold front, rather inactive and not quite marked in terms of near-surface temperatures, was positioned over France and the Iberian Peninsula. *Meteosat* images (Figure 4) show cloudiness ahead of the front with relatively clear skies behind, an indication of the kata phase of the front. The large-scale circulation at 850 hPa is very similar to the surface flow, with cyclonic circulation over the western Mediterranean. The temperature field shows a very well-marked temperature gradient over the eastern part of the Iberian Peninsula associated with the cold front (Figure 7(a)). Moreover, the warm air present over the western Mediterranean, a consequence of the accentuated advection of very warm African air intruding into the region from 25 October, contributed to sharpening this temperature gradient. At 500 hPa, a well-defined trough with a cold core and its axis extended along the Iberian western coast can be identified (Figure 7(b)). The downstream branch of the trough encompassed the whole Iberian Peninsula and the western Mediterranean. At upper levels, 200 hPa (Figure 7(c)), the circulation was also marked by a trough with a quasi-meridional axis extended along the western coast of the Iberian Peninsula. An interesting feature is the jet stream located over the European continent, which is associated with the cold front. According to the four-quadrant model (Carlson, 2012), upward vertical motion would be favoured over the western Mediterranean, as this zone lies under the right entrance quadrant of the jet. Calculation of quasi-geostrophic forcing for upward motion (Hoskins and

 

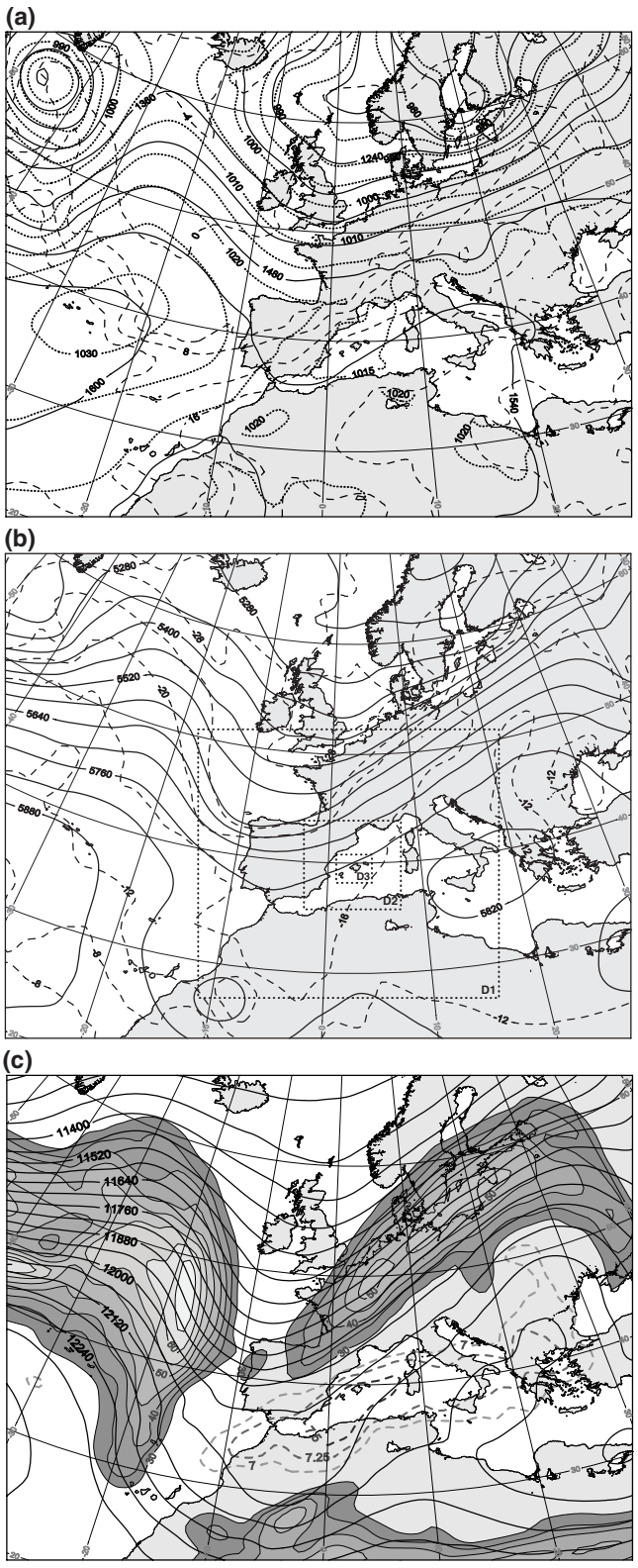


**Figure 7.** Synoptic analysis from the ECMWF on 29 October 2013 at 0000 UTC. (a) Isohypses (solid, in gpm) and temperature (dashed, in °C) at 850 hPa and sea-level pressure (dotted, in hPa). (b) At 500 hPa: isohypses (solid, in gpm) and isotherms (dashed, in °C). (c) At 200 hPa: isohypses (solid, in gpm), wind speed above 30 m s$^{-1}$ (shaded areas) and mean 850–200 lapse rates above 7 °C km$^{-1}$ (dashed lines). In panel (b), the domains D1, D2 and D3 used for the numerical simulations are also depicted.

Pedder, 1980) reveals that synoptic forcing over the region was rather neutral at mid-upper tropospheric levels but positive and intense at low levels (not shown). In addition, very steep lapse rates (exceeding 7.5 °C km$^{-1}$) are also found over this region (Figure 7(c)). Consequently, the synoptic situation on 29 October 2013 was supportive of convection development over the western Mediterranean region.

The atmospheric vertical structure exhibits notable differences between the western Mediterranean (sampled by the Palma de Mallorca radiosounding, Figure 8) and the Iberian Peninsula (Madrid radiosounding). A remarkable feature over Palma on 29 October 2013 at 0000 UTC (Figure 8(a)) is the powerful thermal (or capping) inversion, due to the warm air overriding a shallow layer of moist and cooler air present at the lowest levels (below 950 hPa); the warm layer exhibits very low humidity (the dew-point depression at 950 hPa is 20 °C). A nearly dry adiabatic lapse rate extends above the inversion and up to 530 hPa. Mid-tropospheric air is cold enough to yield latent instability for the surface parcels and the resulting Convective Available Potential Energy (CAPE) value is large (1461 J kg$^{-1}$), although the CIN is also large (370 J kg$^{-1}$) and the level of free convection (LFC) is quite high (730 hPa). A profile of potential or convective instability (i.e. $\theta_e$ decreasing with height) is identified throughout the lowest 100–150 hPa of the sounding and the profile is quasi-neutral above this layer (see Table 1). The concurrent hodograph indicates only slight helicity in the lower troposphere; under some assumptions regarding the wind field (see Tudurí and Ramis, 1997), this is equivalent to weak warm-air advection in the environment. Precipitable water was low (24 mm) when compared with values commonly observed in heavy precipitation cases of the western Mediterranean region, a consequence of the low-tropospheric dry layer. The profile of this sounding and its characteristics conform with a structure referred to as a 'lid' (Farrell and Carlson, 1989), known to be conducive to the development of intense thunderstorms if the low-level parcels can break the inversion and reach the LFC. Moreover, this kind of environment favours the organization of convection (if any) in a few cells. The lid structure results from the northward advection of African air that persisted from 25 October; in these conditions, the warm and dry African air mass settles over the surface layer of moist and cooler air that remains in contact with the Mediterranean Sea.

In Madrid (not shown), the vertical profile is completely different. There is a weak inversion at around 800 hPa that corresponds to the frontal-zone-associated inversion. Above the front, the air is very dry and is advected ahead of the front by the strong winds present over the frontal dome (another indication of a kata-type front). There is no latent instability. Simultaneous soundings from Murcia and Barcelona show a slight thermal inversion at low levels and the presence of dry air above, but this structure had much less amplitude than the one observed over Mallorca. Both soundings reveal latent instability, with CAPE values between 300 and 450 J kg$^{-1}$ and LFC between 700 and 660 hPa.

The situation evolved in such a way that the sounding from Palma de Mallorca 12 h later (i.e. on 29 October 2013 at 1200 UTC, Figure 8(b)) does not show the strong low-level inversion and dry layer, with the lowest 150 hPa now being very humid. Easterly flow at low levels with a low-level jet centred at 950 hPa is now registered and is consistent with the presence of a pressure pattern that advects moist air, which was not acting 12 h before. There is still latent instability, although quite reduced (CAPE is 430 J kg$^{-1}$), the level of free convection is kept high (740 hPa) and the amount of precipitable water increased to 31 mm. At this time, the low-tropospheric layer of potential instability is deeper than at 0000 UTC (Table 1).

Given the vertical structure of the 'representative' sounding at Palma, we can conclude that the convective initiation occurred in an area with important latent instability and a rather high LFC (730–740 hPa). In general terms, the thermodynamical environment can be considered as a dry-line situation, although with a mechanism of formation of the line that differs from the classical one described for the US central plains (e.g. Bluestein and Jain, 1985). Therefore, a strong enough mesoscale forcing would have been operating in this case to enable the low-level parcels to overcome the thermal inversion and reach their LFC. Keeping in mind that the convection started over the sea,

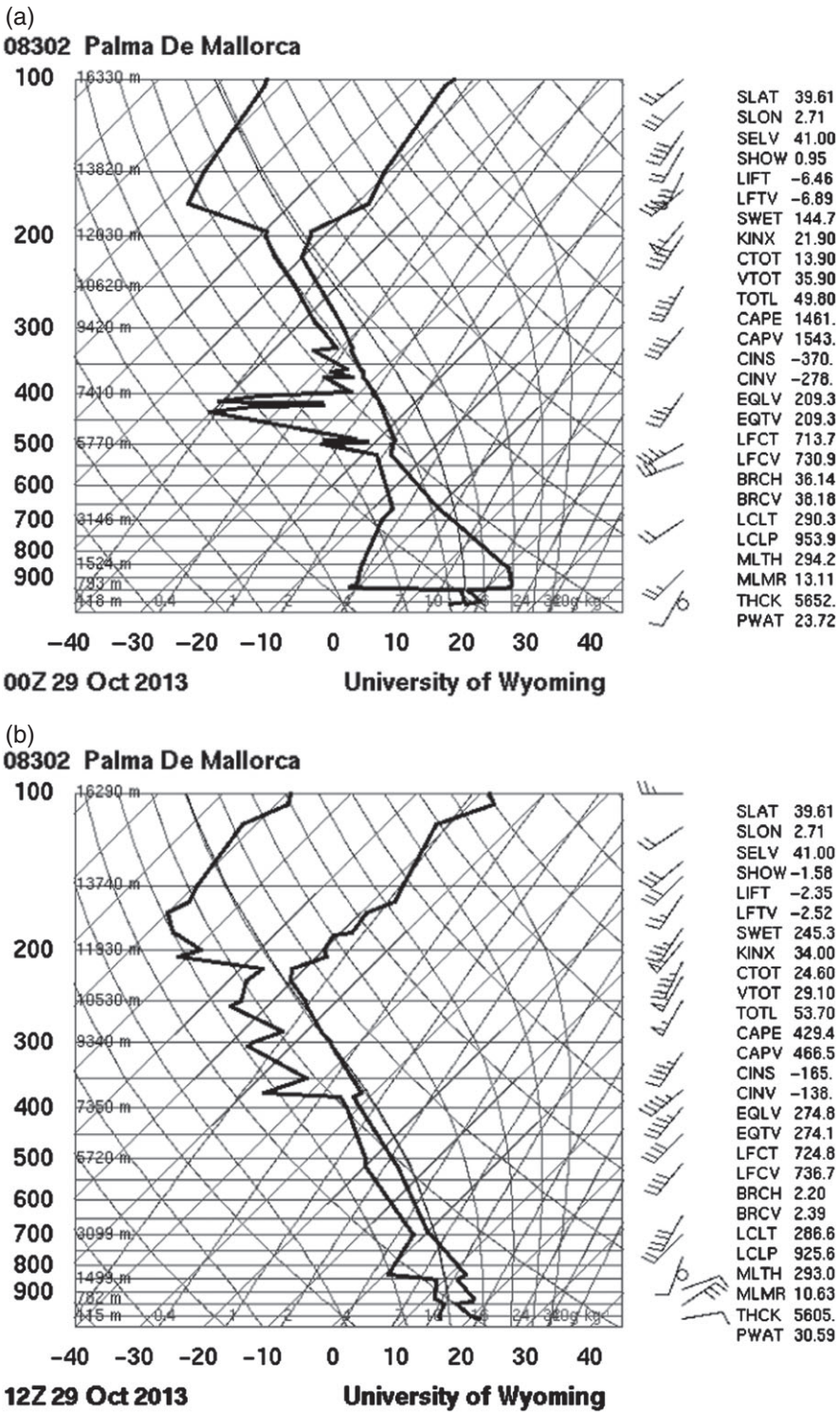


**Figure 8.** Radiosounding from Palma de Mallorca on 29 October 2013, at (a) 0000 UTC and (b) 1200 UTC.

such a mesoscale mechanism must be dynamic, i.e. a low-level convergence zone of sufficient intensity. A hand analysis of surface synoptic observations (SYNOP) data at 0900 UTC (Figure 9(a)) reveals the presence of a depression to the southeast of the Balearic Islands that drives a strong easterly flow towards the area of convective initiation. At the same time, the winds along the Spanish Mediterranean coast took a westerly component. Both elements suggest, indeed, the existence of a convergence zone between the islands and mainland Spain. The data also emphasize the presence of a strong density gradient in the Balearic Sea, more attributable to a humidity gradient than to a thermal front (i.e. the dry-line structure). Indeed, in Mallorca and Ibiza the water-vapour mixing ratio was, respectively, 12 and 13 g kg$^{-1}$, while in Valencia and other locations on the Spanish eastern coast this index was only 7 g kg$^{-1}$. This humidity pattern, in combination with the abovementioned flow organization, implies an accentuated advection of very moist air pointing towards the Spanish coast and especially affecting the region between Mallorca and Ibiza. This preferential region is depicted as a strong packing of the equivalent potential temperature ($\theta_e$) isotherms in Figure 9(a). The convergence line to which the convective initiation is attributed is also sketched, at the location suggested by the satellite images.

The hand surface analysis at 1200 UTC (Figure 9(b)) shows how, after the activation of the precipitation system, the flow of warm and very moist air towards the convective zone still continues, as the wind over the Balearics is strong and from the east. Mixing ratios at Palma and Ibiza are 11 and 14 g kg$^{-1}$, respectively, while in coastal locations of Valencia province the low values (7 g kg$^{-1}$) are maintained. The situation still supports

 

Table 1. Vertical profiles of equivalent potential temperature (K) on 29 October 2013 at 0000 and 1200 UTC, calculated from the Palma de Mallorca radiosoundings.

| Pressure (hPa) | 0000 UTC | 1200 UTC |
|---|---|---|
| 1000 | 333 | 324 |
| 950 | 331 | 323 |
| 900 | 316 | 323 |
| 850 | 317 | 322 |
| 800 | 317 | 315 |
| 750 | 317 | 317 |
| 700 | 317 | 318 |
| 650 | 318 | 317 |
| 600 | 317 | 317 |
| 550 | 316 | 317 |
| 500 | 315 | 317 |
| 450 | 317 | 318 |
| 400 | 320 | 319 |
| 350 | 322 | 321 |
| 300 | 326 | 322 |
| 200 | 335 | 338 |
| 100 | 404 | 414 |

a strong $\theta_e$ gradient along the forward environment of the squall line. It should be noted that for this analysis we took into account not only SYNOP data but also conceptual schemes for the pressure distribution in a squall line (Johnson and Hamilton, 1988) and the observed values of the pressure record presented in Figure 3, assuming that this pressure structure was preserved for several hours. On the other hand, note that the presence of a mesoscale cyclone that acts to drive the moist Mediterranean air mass towards the convective area is consistent with the conceptual scheme proposed by Jansà *et al.* (2001) to link the focused location of convection and heavy rains in the western Mediterranean region with the position of the associated mesoscale low.

## 5. Numerical simulation and sensitivity tests

Simulations of the event were carried out using the non-hydrostatic Fifth-Generation Penn State/NCAR Mesoscale Model (PSU/NCAR MM5) numerical model (Dudhia, 1993; Grell *et al.*, 1995) nested in the European Centre for Medium-Range Weather Forecasts (ECMWF) grid analyses, available at 6 h intervals with a horizontal resolution of about 16 km. The simulations start at 0000 UTC on 29 October 2013 and extend for 24 h, thus fully encompassing the pre-convective environment and the period of development and evolution of the squall line over the Balearic region. The numerical results are downscaled by using the same three domains considered for the operational configuration of the model in our Group (http://mm5forecasts.uib.es; see Figure 7(b)). These domains are connected through two-way interaction and the two inner ones, exploited in this work, cover the Balearic Islands and neighbouring zones with horizontal resolutions of 7.5 and 2.5 km. 30 sigma levels are used in the vertical, with enhanced resolution in the boundary layer (the depth of the lowest layer is approximately 20 m) in order to resolve the turbulent processes better.

Owing to the small-scale and convective nature of the processes involved in this kind of high-impact weather situation, the simulation of a squall line is a challenging task for any model. Firstly, the initial-condition sensitivities very often exert a dominant role. Gallus and Bresch (1997) suggest that one of the challenges in predicting severe weather and heavy precipitation is producing realistic model initial conditions that capture the prior mesoscale environment accurately. Stensrud and Fritsch (1994a, 1994b) showed that the inclusion of initial mesoscale-sized features, not well observed by conventional networks, was a crucial factor in the success of the numerical simulation of a convectively active event in the USA. Similarly, Cohuet *et al.* (2011) showed that mesoscale flows over the Alboran Sea, missed by routine observation networks, were essential for the correct triggering and evolution of the squall line that crossed Mallorca on 4 October 2007. Secondly, numerical representations of mesoscale convective systems would depend strongly on parametrized physical processes like boundary-layer turbulence, cumulus convection and moist microphysics. Here, we examined the sensitivity of the simulation to different combinations of the boundary-layer and explicit cloud schemes (note that no convective parametrization scheme is included in the 2.5 km resolution domain). Specifically, from the variety of options available in MM5, three PBL schemes (Blackadar, Eta and MRF) were combined with four explicit moisture schemes (Dudhia simple ice, Reisner mixed-phase, Reisner graupel and Schultz microphysics). The temporal sequence of the simulated location, intensity and morphology (i.e. linear versus more circular organization) of the convection was, indeed, quite sensitive to the parametrized physics and the best simulation was yielded by the MRF/Reisner mixed-phase combination.

This control experiment (Figure 10) shows remarkable agreement with the radar sequence of the convective system (Figure 5). This points out that the ECMWF analyses used to drive the model have a sufficiently accurate representation of the progressive cold front and prefrontal Mediterranean surface depression (recall Figure 7) and this allows MM5 to resolve the dynamical cascade from synoptic to meso and convective scales adequately. The model captures the genesis of the convective system to the north of Ibiza and its rapid intensification as it approaches the island of Mallorca. As in reality, the system acquires a linear shape during this phase but the model fails in the simulation of the northward extension of the convective line. Also, the modelled squall line is 2 h ahead of observations, such that the simulation at 1100 UTC almost mimics the radar image of 1300 UTC. The tendency observed in the radar towards a more amorphous structure of the MCS as it crossed south Mallorca, followed by the recovery of an elongated bow shape as it left the southeastern coast, is also reproduced accurately by the simulation. In addition, the abovementioned temporal mismatch is progressively reduced in this later phase and, by 1600–1700 UTC, simulated and observed squall lines are almost coincident in location.

The notable intensity of the convective system is evidenced not just in the high precipitation rates simulated through the period but also in the increasing strength of the winds propelled by the storm at the surface. These model-simulated 'mean' winds attain their maximum speed of about 70–80 km $h^{-1}$ when the line is located near the southeastern coast of Mallorca (Figure 10). This is fully consistent with the measured or inferred wind gusts near 100 km $h^{-1}$ and the fact that the severity of the storm was manifested most clearly in this part of the island. Another feature of interest that reconciles the simulation with the available observations is the spatial distribution of the surface wind field relative to the storm. We find a dominant easterly to northeasterly flow ahead of the squall line and a clear tendency to leave northeasterly to northerly winds behind its passage, especially across the southern part of the storm. As we already pointed out in Figure 9(b), such a wind distribution guarantees low-level convergence and continuous feeding of the convective region and is a dynamical consequence of the interaction between the advancing cold front and the maritime flow driven by the prefrontal Mediterranean low.

On the other hand, the fact that the model tends to overemphasize the convective rebuilding of the MCS in its southern sector, to the detriment of its northernmost appendix, means that the system as a whole evolves slightly to the south of the observed track and, as a result, the maximum accumulated precipitation during the episode (Figure 11) is simulated over maritime areas to the southsouthwest of Mallorca. Over land, the rainfall spatial distribution is in reasonable agreement with the observed pattern (Figure 2) and the highest amounts are also found in northern Ibiza and southern Mallorca, although with a significant underestimation of a few tens of mm.

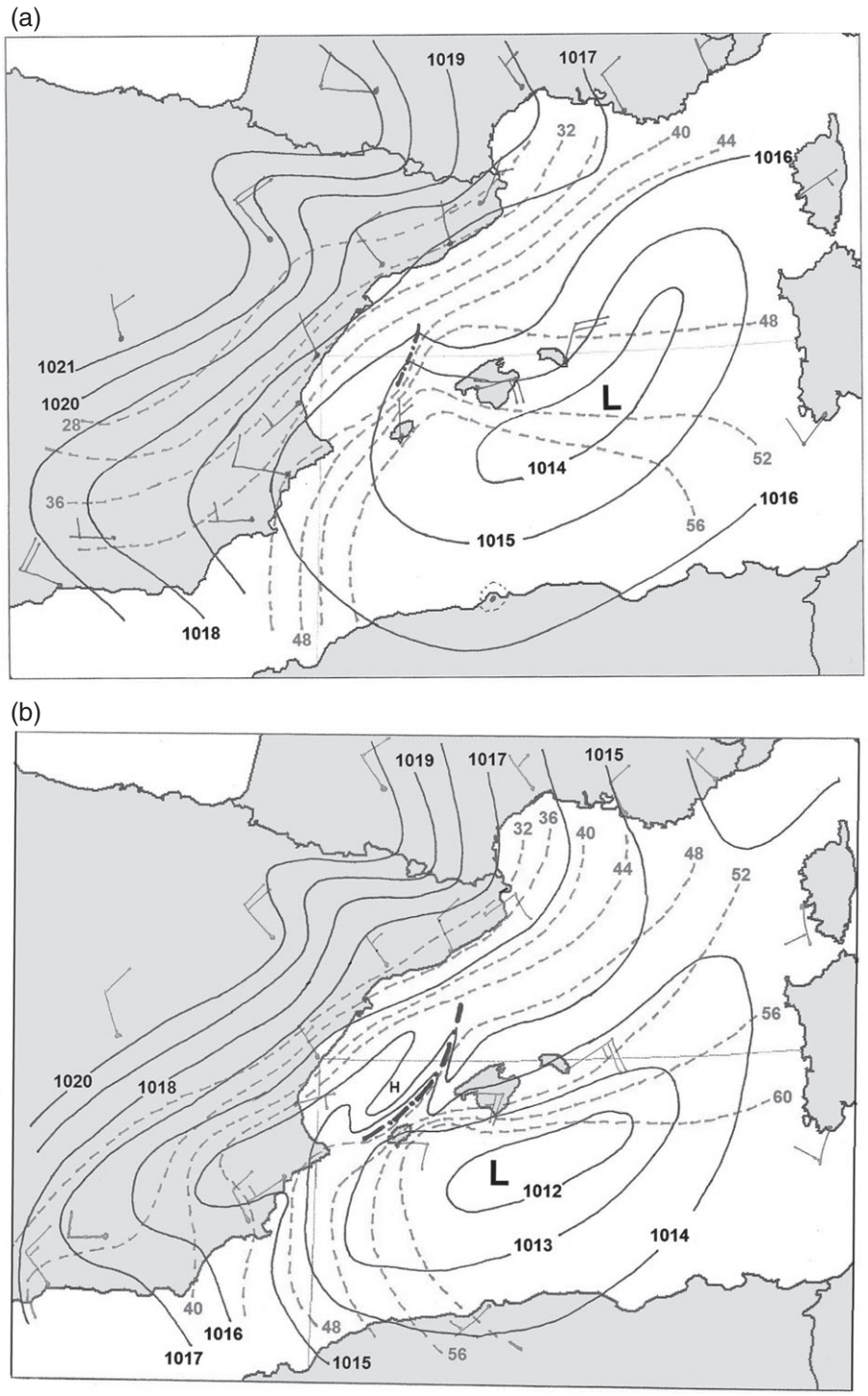


**Figure 9.** Hand analysis of the meteorological situation at the surface on 29 October 2013, at (a) 0900 UTC and (b) 1200 UTC. Continuous lines: isobars (hPa). Dashed lines: equivalent potential temperature isotherms (°C). Plotted winds follow the classical conventions of synoptic meteorology (knots). The dash–dotted line represents the convergence line inferred from satellite images. The data used for the analysis come from the SYNOP stations, located at the wind-barb heads.

### *5.1. Mesoscale environment and s quall-line structure*

As a complement to the observational analysis presented in previous sections, the successful simulation of the case allows us to investigate in further detail the mesoscale factors involved in the triggering, maintenance and linear organization of the convection. An analysis of the internal structure of the squall line is also possible, through the analysis of transverse vertical sections of the MCS.

Figure 12 shows composites of mesoscale ingredients at 0800, 1200 and 1600 UTC as simulated in the second domain of the control experiment. These plots summarize, through a few fields, key necessary factors for the triggering and sustainment of convection (Doswell *et al.*, 1996). Firstly, the latent and convective instability of the low-level warm and moist Mediterranean air is examined through the $\theta_e$ field at 1000 hPa (CAPE for the surface parcel and potential instability in the lowest 150 hPa almost perfectly overlap regions of surface $\theta_e$ above 44°C); secondly, moisture supply and low-level convergence (i.e. upward motion) are illustrated through the horizontal water-vapour flux integrated across the low troposphere (note in the figures how the indicated regions of significant upward motion at 850 hPa are collocated with convergence lines of the moisture flux vectors); finally, we include the sea-level pressure field in order better to understand its role in the organization of the low-level airstreams. Interestingly, the model-derived composites are quite consistent with the subjective analyses presented in Figure 9, even though these hand analyses were derived independently and solely using the few SYNOP reports available around the western Mediterranean.

 

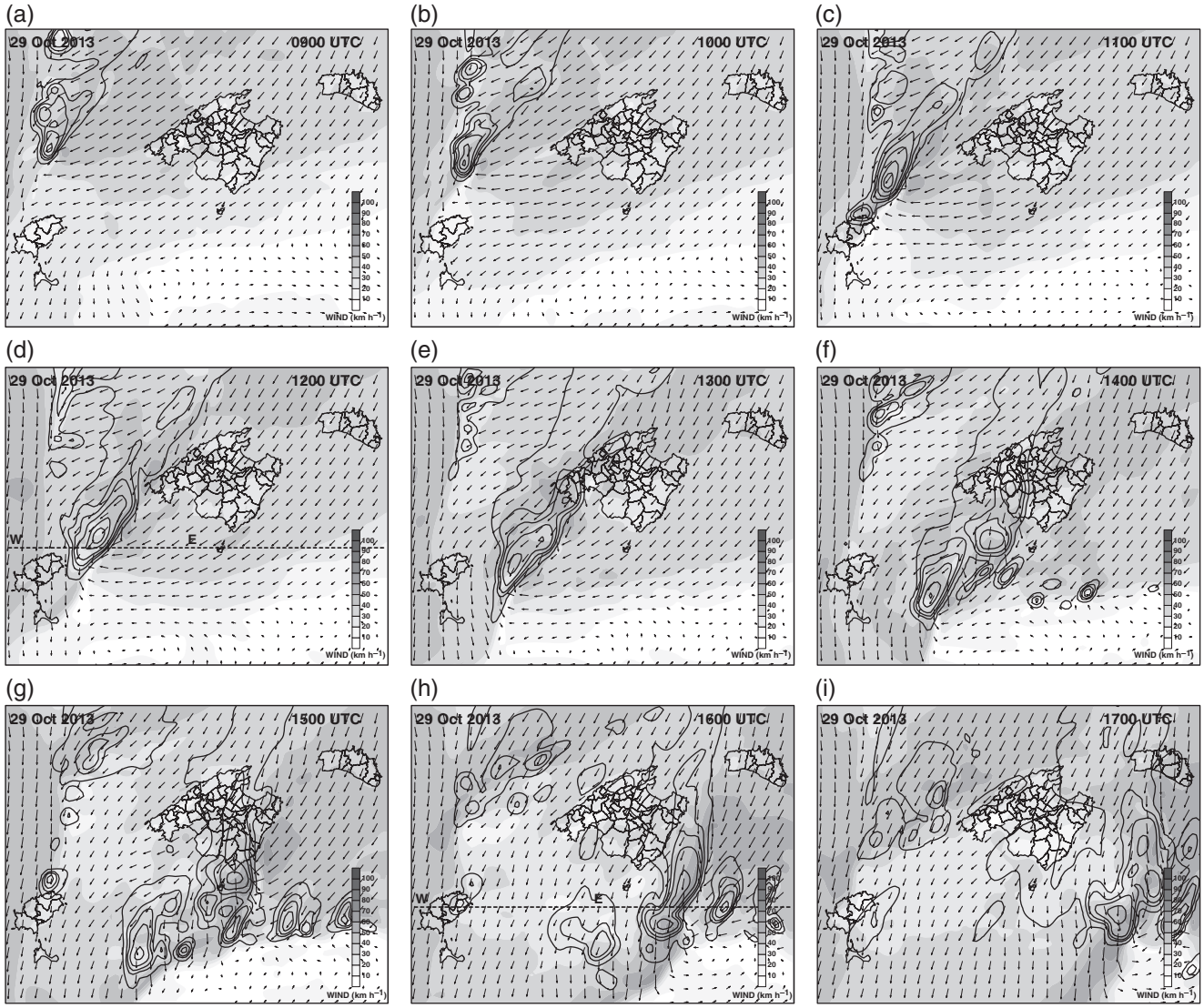


**Figure 10.** (a)–(i) Temporal sequence in the control simulation of the fields: 30 min precipitation (contour lines, with intervals 1, 5, 10, 20, 40 and 60 mm), surface wind vectors and surface wind speed (shaded, in km $h^{-1}$ according to scale). These outputs belong to the domain D3 (2.5 km resolution) shown in Figure 7(b). Lines W–E indicated at 1200 and 1600 UTC correspond to the vertical cross-sections analyzed in the text.

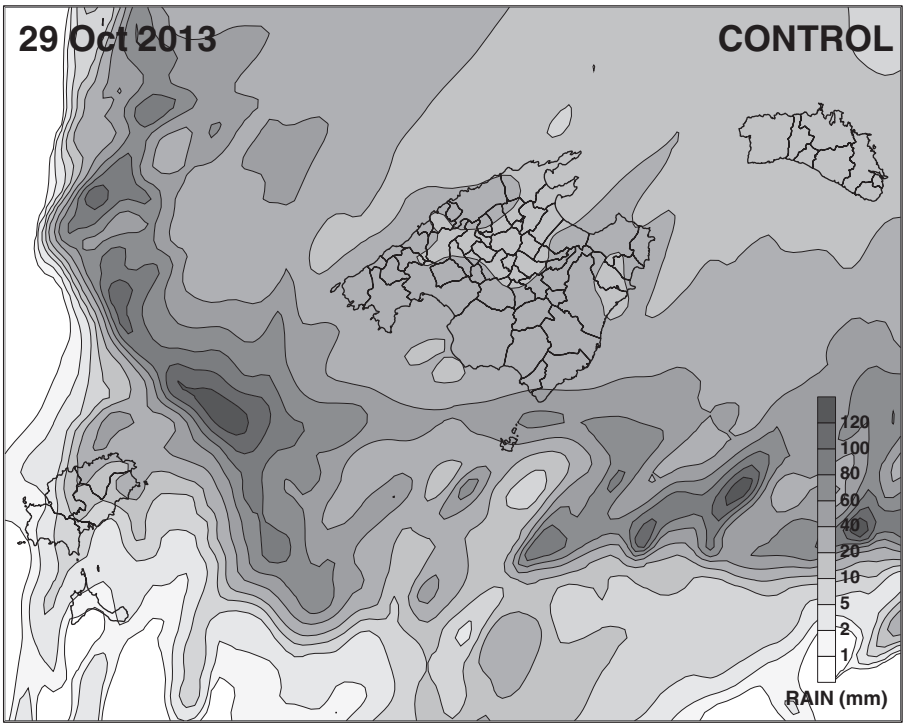


**Figure 11.** Total accumulated precipitation (mm in 24 h, according to scale) in the control simulation for the D3 domain (2.5 km resolution, shown in Figure 7(b)).

 

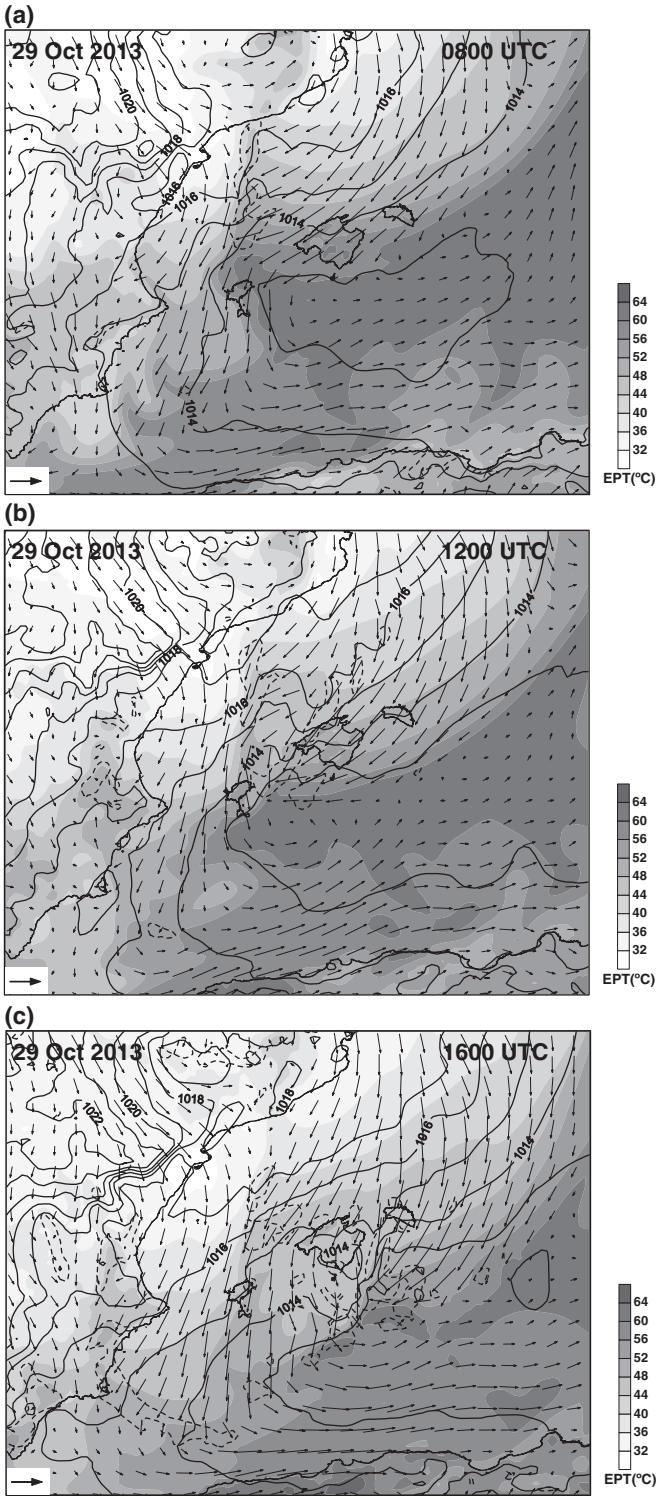


**Figure 12.** Mesoscale ingredients accompanying (a) initiation (0800 UTC) and (b) and (c) evolution (1200 and 1600 UTC) of the simulated convective system. Fields shown are the 1000–850 hPa vertically integrated water-vapour flux (vectors; reference vector corresponds to 200 kg m$^{-1}$ s$^{-1}$), equivalent potential temperature at 1000 hPa (shaded, in °C according to scale), sea-level pressure (hPa, thin contour lines) and regions of upward motion at 850 hPa greater than 15 cm s$^{-1}$ (thick dashed contour). These outputs belong to the domain D2 (7.5 km resolution) shown in Figure 7(b).

By comparison of Figure 12 against Figure 10, it is clear that the MCS developed and evolved along a boundary separating high-$\theta_e$ Mediterranean air from a cooler and drier air mass that advanced from the northwest in connection with the cold front passage. This boundary is very accentuated to the northwest of the Balearics during the initiation phase of the system (0800 UTC, Figure 12(a)), owing to a pocket of $\theta_e$ rich air that extends northwards of Ibiza. Convection is triggered along the northernmost tip of this unstable air, where northerly and northeasterly low-level currents converge. The superposition of low-level moisture flux convergence and upward motion in a region of enough instability is not only the mechanism that initiates the convection, but also the factor that drives and feeds the system during its journey to the southeast, helping to maintain its linear structure (see the composites at 1200 and 1600 UTC; Figure 12(b) and (c), respectively). In this sense, the low-pressure zone centred to the south of the islands and the concomitant acceleration of the northeasterly flow along its northern flank become instrumental in supporting and enhancing this convergence just ahead of the advancing cold front. Of course, once the convection initiates, low-level convergence and vigorous lifting of the convectively unstable air along the forward flank of the squall line are further stimulated by the MCS internal circulation. This notion becomes most clear at 1200 and 1600 UTC, when the system is fully developed, but attempting to isolate the convective-scale forcing from the external mesoscale factors based on the simulation fields becomes impractical.

Figure 13 illustrates the internal structure of the simulated convective system at 1200 UTC, when it was about to reach Mallorca, and at 1600 UTC, when it had already passed the island (recall Figure 10). At 1200 UTC, a single and vigorous convective line is observed (Figure 13(a)) and this follows the conceptual model of a squall system closely (e.g. Johnson and Hamilton, 1988; Houze *et al.*, 1989). Pre-squall meso-low, meso-high and wake low are all identified at the surface. Along the eastern flank of the meso-high, the storm is ingesting the Mediterranean high $\theta_e$ air found in its forward environment, as evidenced by the intense convective updraught (the maximum vertical velocity at this time is 20 m s$^{-1}$) and the deep plume of nearly-conserved $\theta_e$ that connects the boundary layer with the upper troposphere. This plume is tilted westwards; the characteristic downdraught of evaporatively cooled air that spreads over the meso-high is clearly found beneath it. Compensating subsidence in the environment around the storm can also be inferred at mid-tropospheric levels, as well as the genesis and propagation in the forward direction of gravity waves from the overshooting region. The aforementioned anchoring of the storm to the low-level $\theta_e$ boundary during the episode becomes very clear in Figure 13: the system propagates eastward into the region of latent and convective instability (high $\theta_e$ values at the PBL, which decrease strongly with height), leaving behind the cooler and much more stable air mass that accompanies the cold front. The cross-section at 1600 UTC (Figure 13(b)) shows a more complex structure: in addition to the main convective line, other dissipating cells are visible to the west of the line, whereas to the east new convective cells help to release the convective instability still present in the environment.

### *5.2. Role of local and regional factors in convective initiation and evolution*

Several numerical studies of intense Mediterranean convective events conclude that local factors, such as diurnal diabatic heating and regional topography, can become under some circumstances instrumental for the destabilization of the air mass and for the convective initiation or intensification through alterations of the mesoscale flow (e.g. Homar *et al.*, 2003; García-Ortega *et al.*, 2007). The 29 October 2013 storm was essentially a maritime phenomenon, but since the Balearic orography is so prominent (especially in Mallorca, where the Tramuntana range has several peaks above 1000 m) and the northern part of the squall line moved over land areas, it is reasonable to analyze the possible role of the local topography. Accordingly, we flattened the Islands orography to zero elevation in a new simulation of the case. Except for a slightly faster eastward progression and a weaker intensity over southern Mallorca in this experiment, the resulting squall line evolves almost identically to the control run. The accumulated precipitation field, very similar to the control accumulations except in the proximity of the largest island (compare Figures 11

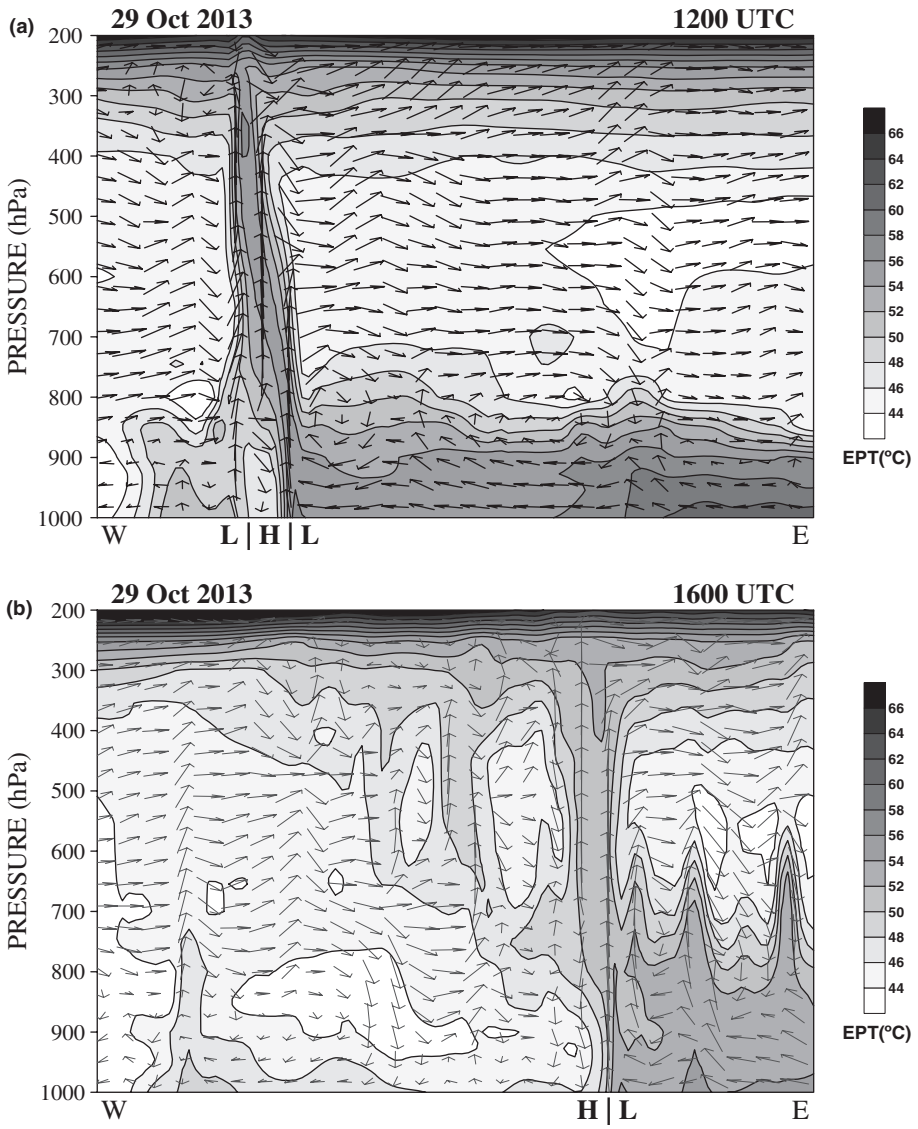


**Figure 13.** West–east vertical cross-section of the simulated convective system at (a) 1200 UTC and (b) 1600 UTC, along the lines indicated in Figure 10. The cross-section shows the equivalent potential temperature (°C, according to scale), transverse circulation (vectors, defined by the zonal and vertical components of the wind; a logarithmic scaling of magnitude is used) and storm-scale highs and lows identified at the surface near the position of the convective system (H and L symbols).

and 14(a)), summarizes the relative insensitivity of this case to the local topography.

However, when the entire orography of the computational domains is removed, the resulting effects are more profound (Figure 14(b)): no linear convective system is formed to the west of Mallorca and intense convection eventually occurs, but over Ibiza and the south Balearic sea during the afternoon hours. We thus conclude that the orographic action was crucial for the genesis and linear organization of the convective system during the early morning of 29 October and this is confirmed by examining the mesoscale ingredients at 0800 UTC (Figure 15(a)), to be compared with the control run (Figure 12(a)): the elongated convergence zone of the low-level flow between Ibiza and Catalonia is absent in the non-orographic simulation. This convergence line was largely associated with the enhanced easterly component of the Mediterranean airstream and enhanced westerly component of the Iberian current imposed by the coastal troughing in the lee of the Iberian peninsula and the pressure perturbations provoked by the Spanish mountain ranges. Such a role of regional orography in generating or enhancing the low-level convergence of an unstable air mass recalls other studied convective cases from eastern Spain, in which a similar remote action, attributed to the African Atlas mountain range, was numerically proven (e.g. Homar *et al.*, 1999; Romero *et al.*, 2000).

Other numerical studies of heavy precipitation events have emphasized the role of evaporation from the Mediterranean Sea as an amplification factor of the responsible precipitating structure, helping to feed and sustain the system to the point of breaking the threshold between ordinary rainfalls and extreme coastal accumulations (e.g. Ramis *et al.*, 1998; Duffourg and Ducrocq, 2011). Recall that these events tend to occur in late summer and autumn, when the sea-surface temperature (SST) is at its highest value in the region and the recharging of the lower atmosphere through the surface moist fluxes, even during a few hours, is very effective. We repeated the numerical experiment of the convective storm, but this time removing the evaporation from the sea during the course of the simulation. The results are certainly interesting and reflect an extreme sensitivity of the 29 October 2013 episode to the latent heat fluxes (Figure 14(c)). Not only is the efficiency of the episode reduced, as evaluated, for instance, through the accumulated rainfall, which becomes much less over the maritime zones, but the character of the precipitation system itself changes drastically when the evaporation is absent. Instead of intense, localized convection organized in the form of an advancing and self-sustained line, the convective energy release becomes weaker and widespread over the region and there are no signs of convection organization or severity. Such a strong influence of evaporation on the convective mode of the case suggests a complex link between this physical factor and the dynamics that would be crucial to enable convective initiation in the proper place and time for the squall line to occur.

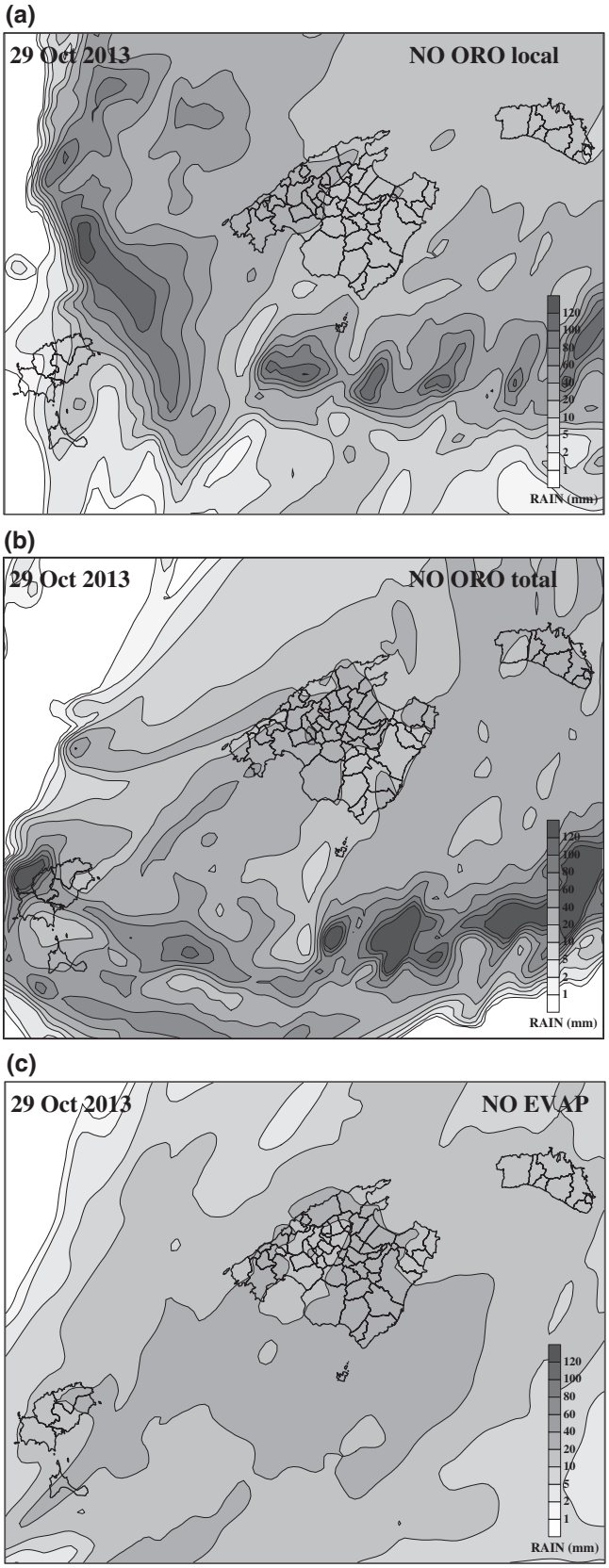


**Figure 14.** As in Figure 11, but for the simulations: (a) without local orography, (b) without total orography and (c) without evaporation from the sea.

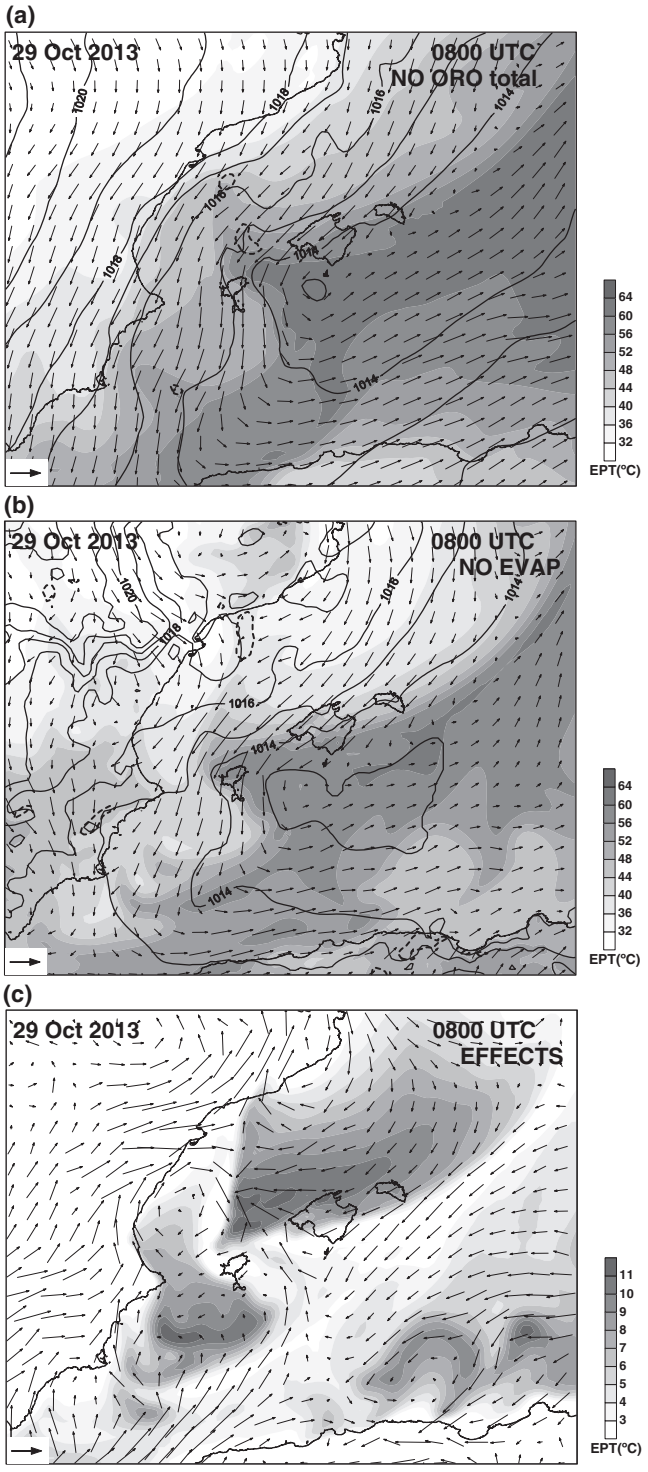


**Figure 15.** As in Figure 12(a), but for the simulations: (a) without total orography and (b) without evaporation from the sea. Panel (c) summarizes the effect of the orography on the 1000–850 hPa vertically integrated water-vapour flux (vectors; reference vector corresponds to 100 kg m$^{-1}$ s$^{-1}$) and the effect of evaporation on the equivalent potential temperature at 1000 hPa (shaded, in °C according to scale); see text.

It is worth investigating this idea and in Figure 15(b) we redraw the mesoscale composite at the initiation phase of the convective system (as in Figure 12(a)), except for the simulation without evaporation from the sea. The most outstanding feature compared with the control experiment is the general decrease of low-level $\theta_e$ – and thus of latent and convective instability – found across the domain. This reduction is especially accentuated to the north and west of Mallorca, to the extent that dynamical forcing and thermodynamic ingredients do not combine optimally this time, convection is not triggered to the west of Mallorca and the passage of the cold front becomes largely unproductive. Our main findings regarding the crucial roles of total orography and evaporation from the sea are summarized in Figure 15(c) as the effects (by subtraction of the perturbed experiments from the control run) of the former factor on the low-level moisture flux and the latter on the surface $\theta_e$. Clearly, the initiation and early linear organization of the 29 October convective storm are attributable to the low-level convergence stimulated by the topography to the north of Ibiza along the western boundary of a moisture-enriched air mass.

Finally, the crucial role of surface latent heat fluxes during the first hours of 29 October in guaranteeing enough moisture content of the low-level parcels approaching the Balearics from the northeast motivates a re-examination of the case from the point of view of its sensitivities to changes in Mediterranean SSTs. According to the ECMWF analyses, the SST during the last days of October 2013 was about 22–23 °C in the western Mediterranean area, with a sharp gradient in the northern part of the basin towards the 19 °C values found at the French coastal zone. Six new simulations in which the SST was decreased and increased uniformly by fixed amounts of 1, 2 and 3 °C were compared against the control experiment. These tests are of both academic and practical interest, because uncertainties in SST analyses might reach several tenths of a degree (Thiébaux *et al.*, 2003) and the examined range of values is also compatible with actual observed SST anomalies and intraseasonal trends and even with the expected warming of the Mediterranean sea associated with climate change (Somot *et al.*, 2008). Results indicate that the 29 October situation was close to a critical point, since cooling the SST by as little as 1 °C would not have produced the squall line; any intense convection would have been released some hours later and further south (compare Figure 16(a) with Figure 11). This result is confirmed and amplified in the experiments with 2 and 3 °C SST reduction (not shown), confirming that the low-level airstreams converging to the west of the Balearics ahead of the cold front were initially too dry. Cooling the Mediterranean implies that these parcels need a longer fetch over the water body before sufficient latent and convective instability can be accumulated and the capping inversion effectively eroded. In contrast, in the experiments with a warmer Mediterranean, squall lines are invariably simulated and these become increasingly faster, more intense – and violent at the surface – and more displaced towards the north of Mallorca as the SST increases (see the case of SST +3 °C in Figure 16(b)).

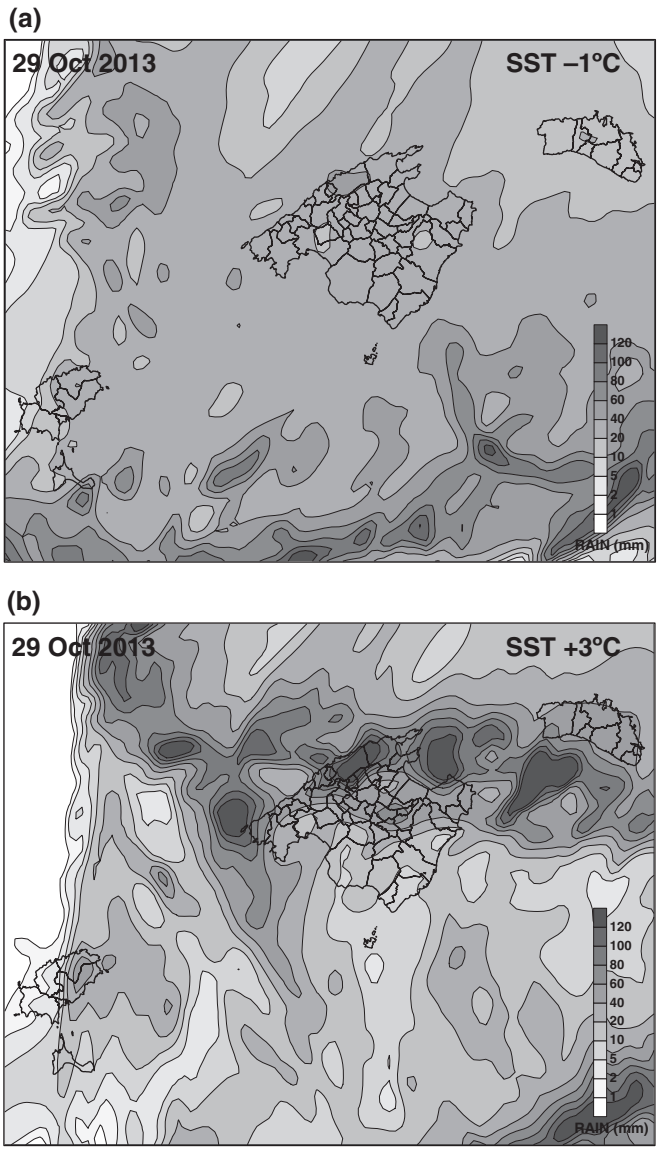


**Figure 16.** As in Figure 11, but for the simulations with modified SST: (a) SST −1 °C, (b) SST +3 °C.

## 6. Conclusions

The analysis of the severe convective storm of 29 October 2013 in the Balearic Islands using different sources of data, from observational to numerically simulated products, helped us to understand the synoptic and mesoscale mechanisms that led to the development, intensification and propagation of the squall line. These products were also useful to explore the morphology and internal dynamics of the storm and become instructive with regard to predictability assessments. Although the analysis of a single case study narrows, in principle, the general applicability of the lessons derived in this article, findings are substantial enough to offer forecasters and scientists a better anticipation and understanding of many other situations of organized convective systems forced over maritime areas.

At the synoptic scale, the upper-level pattern was broadly similar to many other situations associated with moist convective developments over the western Mediterranean region during the fall, i.e. a pattern characterized by a cold trough irrupting into the region from the Atlantic. However, contrary to the conceptual model of heavy precipitation in eastern Spain linked to quasi-stationary MCSs, which demand the presence of a slow-moving precursor trough aloft (possibly a cut-off cyclone) and marked warm and moist air advection at low levels favoured by a surface depression, the synoptic situation on 29 October 2013 was governed by a progressive upper-level trough and the simultaneous advance of a surface cold front. The resulting convection started entirely over the sea, was readily organized as a linear structure (at times severe) and moved very fast over the Islands territory. This kind of phenomenon is unusual, while the passage of cold fronts over the Balearics is a common feature in any season excepting the full summer; thus some special meteorological conditions had to concur on 29 October 2013. Unique features in the case studied were (i) the capping of the low-level moist Mediterranean layer with dry and warm African air during the previous days and (ii) the development of a significant low-pressure area over the Mediterranean ahead of the cold front. The former feature contributed to producing large temperature lapse rates between low and high tropospheric levels and to inhibiting the release of the latent and convective instability present in the environment until enough mesoscale lifting was available. The prefrontal low was not only relevant in destabilizing the environment and guaranteeing the influx of Mediterranean air into the precipitation system, once generated; it was instrumental in defining a quasi-linear convergence zone in between the archipelago and mainland Spain just ahead of the pushing cold front, where the convective system could be initiated and organized. In fact, the convective system remained during its entire life cycle rooted in a dynamical boundary separating unstable high-$\theta_e$ Mediterranean air from a stable low-$\theta_e$ air mass associated with the progressive cold front.

However, some striking findings we obtained during the numerical investigation of the case demonstrate that strictly atmospheric processes were not enough to concatenate the sequence of kinematic and thermodynamic processes behind the convective storm genesis and evolution. The cooperation between synoptic/sub-synoptic circulation systems and two boundary factors commonly analyzed in the western Mediterranean region, owing to either its complexity (topography) or its role as a major local moisture source (evaporation from the Mediterranean), was shown to be crucial for the 29 October 2013 event. Topographic

modifications of the low-level flow enhanced the maritime convergence line along which the convective system developed. Meanwhile, the evaporation allowed the low-level parcels to reach the critical water-vapour content necessary to release and sustain the convection.

Finally, the reasonably accurate simulation of the case at different spatial scales points to the aptitude of the current operational analyses, even in a region with low-density observational data such as the Mediterranean, towards forcing serviceable fine-grid forecasts before potentially dangerous convective systems. However, our study also shows a significant sensitivity of the simulation to the choice of model physical parametrizations and to external parameters like the SST. In addition, complex interactions between convective-scale processes and mesoscale ingredients when the simulated storm is fully developed can easily be anticipated in light of our results. These and other conceivable uncertainties would naturally affect, even under optimum initial atmospheric states, the credibility in the numerical outcomes of deterministic forecasts with regard to the detailed timing and location of deep convection and the severe weather threat. We are currently working on implementing probabilistic frameworks based on ensemble prediction systems aimed at meso and convective scales. The 29 October 2013 episode will undoubtedly become an excellent test bed for assessing the value of such types of system.

## Acknowledgments

Precipitation data for the Balearic Islands, as well as radar images, were provided by Agencia Estatal de Meteorología of Spain (AEMET). The authors acknowledge AEMET and the HyMeX database for supplying the surface 10 min data used within the study. Satellite images were obtained from *EUMETSAT*, while the analyzed soundings were retrieved from the University of Wyoming. The photograph of the storm was kindly provided by J. F. Mas. This research is framed within the CGL2011-24458 Spanish project and it has also been partially funded by the Government of the Balearic Islands through the project 7/2011 of the 'Conselleria d'Educació, Cultura i Universitats'.

## References

Barceló M. 1991. Per una aproximació a la climatologia de Mallorca baixmedieval a través dels textos històrics. *Boll. Soc. Arqueol. Lull.* **47**: 123–140.

Bluestein HB, Jain MH. 1985. Formation of mesoscale lines of precipitation: Severe squall lines in Oklahoma during the spring. *J. Atmos. Sci.* **42**: 1711–1732.

Carlson TN. 2012. *Mid-latitude Weather Systems.* Penn State University Press: University Park, PA.

Cohuet JB, Romero R, Homar V, Ducrocq V, Ramis C. 2011. Initiation of a severe thunderstorm over the Mediterranean Sea. *Atmos. Res.* **100**: 603–620.

Doswell CA III, Brooks HE, Maddox RA. 1996. Flash flood forecasting: An ingredients-based methodology. *Weather and Forecasting* **11**: 560–581.

Ducrocq V, Bougeault P. 1995. Simulation of an observed squall line with a meso-beta hydrostatic model. *Weather and Forecasting* **10**: 380–399.

Dudhia J. 1993. A non-hydrostatic version of the Penn State/NCAR mesoscale model: Validation tests and simulation of an Atlantic cyclone and cold front. *Mon. Weather Rev.* **121**: 1493–1513.

Duffourg F, Ducrocq V. 2011. Origin of the moisture feeding the heavy precipitation systems over Southeastern France. *Nat. Hazards Earth Syst. Sci.* **11**: 1163–1178.

Farrell RJ, Carlson TN. 1989. Evidence for the role of the lid and underrunning in an outbreak of tornadic thunderstorms. *Mon. Weather Rev.* **117**: 857–871.

Fernández C, Gaertner MA, Gallardo C, Castro M. 1995. Simulation of a long-lived meso-$\beta$ scale convective system over the Mediterranean coast of Spain. Part I: Numerical predictability. *Meteorol. Atmos. Phys.* **56**: 157–179.

Gallagher FW III, Beasley WH, Bohren CF. 1996. Green thunderstorms observed. *Bull. Am. Meteorol. Soc.* **77**: 2889–2897.

Gallus WA, Bresch JF. 1997. An intense small-scale wintertime vortex in the midwest United States. *Mon. Weather Rev.* **125**: 2787–2807.

García-Ortega E, Fita L, Romero R, López L, Ramis C, Sánchez JL. 2007. Numerical simulation and sensitivity study of a severe hail-storm in northeast Spain. *Atmos. Res.* **83**: 225–241.

Gayà M. 2011. Tornadoes and severe storms in Spain. *Atmos. Res.* **100**: 334–343.

Grell G, Dudhia J, Stauffer DR. 1995. 'A description of the fifth-generation of the Penn State/NCAR mesoscalemodel (MM5)', NCAR Technical Note NCAR/TN-398+STR. NCAR Library: Boulder, CO.

Homar V, Ramis C, Romero R, Alonso S, García-Moya JA, Alarcón M. 1999. A case of convection development over the western Mediterranean Sea: A study trough numerical simulation. *Meteorol. Amos. Phys.* **71**: 169–188.

Homar V, Gayà M, Ramis C. 2001. A synoptic and mesoscale diagnosis of a tornado outbreak in the Balearic Islands. *Atmos. Res.* **56**: 31–55.

Homar V, Gayà M, Romero R, Ramis C, Alonso S. 2003. Tornadoes over complex terrain: An analysis of the 28th August 1999 tornadic event in eastern Spain. *Atmos. Res.* **67–68**: 301–317.

Hoskins BJ, Pedder MA. 1980. The diagnosis of middle latitude synoptic development. *Q. J. R. Meteorol. Soc.* **106**: 707–719.

Houze RA Jr, Rutledge SA, Biggerstaff MI, Smull BF. 1989. Interpretation of Doppler weather radar displays of midlatitude mesoscale convective systems. *Bull. Am. Meteorol. Soc.* **70**: 608–619.

Jansà A, Genovés A, Picornell MA, Campins J, Riosalido R, Carretero O. 2001. Western Mediterranean cyclones and heavy rain. Part 2: Statistical approach. *Meteorol. Appl.* **8**: 43–56.

Johns RH. 1993. Meteorological conditions associated with bow echo development in convective storms. *Weather and Forecasting* **8**: 294–299.

Johnson RH, Hamilton PJ. 1988. The relationship of surface pressure features to the precipitation and airflow structure of an intense midlatitude squall line. *Mon. Weather Rev.* **116**: 1444–1473.

Malguzzi P, Grossi G, Buzzi A, Ransi R, Buizza R. 2006. The 1966 'century' flood in Italy: A meteorological and hydrological revisitation. *J. Geophys. Res. Atmos.* **111**: D24, doi: 10.1029/2006JD007111.

Przybylinski RW. 1995. The bow echo: Observations, numerical simulations, and severe weather detection methods. *Weather and Forecasting* **10**: 203–218.

Ramis C, Arús J, López JM, Mestres AM. 1997. Two cases of severe weather in Catalonia (Spain). An observational study. *Meteorol. Appl.* **4**: 207–217.

Ramis C, Romero R, Homar V, Alonso S, Alarcón M. 1998. Diagnosis and numerical simulation of a torrential precipitation event in Catalonia (Spain). *Meteorol. Atmos. Phys.* **69**: 1–21.

Ramis C, López JM, Arús J. 1999. Two cases of severe weather in Catalonia (Spain). A diagnostic study. *Meteorol. Appl.* **6**: 11–27.

Ramis C, Romero R, Homar V. 2009. The severe thunderstorm of 4th October 2007 in Mallorca: An observational study. *Nat. Hazards Earth Syst. Sci.* **9**: 1237–1245.

Ramis C, Homar V, Amengual A, Romero R, Alonso S. 2013. Daily precipitation records over mainland Spain and the Balearic Island. *Nat. Hazards Earth Syst. Sci.* **13**: 2483–2491.

Romero R, Ramis C, Alonso S. 1997. Numerical simulation of an extreme rainfall event in Catalonia: Role of orography and evaporation from the sea. *Q. J. R. Meteorol. Soc.* **123**: 537–559.

Romero R, Guijarro JA, Ramis C, Alonso S. 1998a. A 30 year (1964–1993) daily rainfall data base for the Spanish Mediterranean regions: First exploratory study. *Int. J. Climatol.* **18**: 541–560.

Romero R, Ramis C, Alonso S, Doswell CA III, Stensrud DJ. 1998b. Mesoscale model simulation to three heavy precipitation events in the western Mediterranean region. *Mon. Weather Rev.* **126**: 1859–1881.

Romero R, Doswell CA III, Ramis C. 2000. Mesoscale numerical study of two cases of long-lived quasistationary convective systems over eastern Spain. *Mon. Weather Rev.* **128**: 3731–3751.

Sánchez JL, Fernández MV, Fernández JT, Tudurí E, Ramis C. 2003. Analysis of mesoscale convective systems with hail precipitation. *Atmos. Res.* **67–68**: 573–588.

Somot S, Sevault F, Déqué M, Crépon M. 2008. 21st century climate change scenario for the Mediterranean using a coupled atmosphere–ocean regional climate model. *Global Planet. Change* **63**: 112–126.

Stensrud DJ, Fritsch JM. 1994a. Mesoscale convective systems in weakly forced large-scale environments. Part II: Generation of a mesoscale initial condition. *Mon. Weather Rev.* **122**: 2068–2083.

Stensrud DJ, Fritsch JM. 1994b. Mesoscale convective systems in weakly forced large-scale environments. Part III: Numerical simulations and implications for operational forecasting. *Mon. Weather Rev.* **122**: 2084–2104.

Thiébaux J, Rogers E, Wang W, Katz B. 2003. A new high-resolution blended real-time global sea-surface temperature analysis. *Bull. Am. Meteorol. Soc.* **84**: 645–656.

Tudurí E, Ramis C. 1997. The environments of significant convective events in the western Mediterranean. *Weather and Forecasting* **12**: 294–306.

Wang PK. 2002. The Kansas green thunderstorm of 4 October 1998. *Bull. Am. Meteorol. Soc.* **83**: 355–357.

 